



ChemComm

**Salt-Rich Solid Electrolyte Interphase for Safer High-Energy-Density Li Metal Batteries with Limited Li Excess**

Journal:	<i>ChemComm</i>
Manuscript ID	CC-COM-04-2020-002481.R2
Article Type:	Communication

SCHOLARONE™  
Manuscripts

## COMMUNICATION

## Salt-Rich Solid Electrolyte Interphase for Safer High-Energy-Density Li Metal Batteries with Limited Li Excess

Received 00th January 20xx,  
Accepted 00th January 20xx

Shouyi Yuan,<sup>[1]</sup> Junwei Lucas Bao,<sup>[2]</sup> Nan Wang,<sup>[1]</sup> Xiang Zhang,<sup>[1]</sup> Yonggang Wang,<sup>[1]</sup> Donald G. Truhlar\*,<sup>[2]</sup> Yongyao Xia\*<sup>[1]</sup>

DOI: 10.1039/x0xx00000x

**We propose a carbonate-based electrolyte optimized with dual cations and ionic liquid for high-efficiency Li metal batteries with high-voltage cathode. An average coulombic efficiency of Li deposition of 99.6% is achieved due to the salt-rich solid electrolyte interphase and Na guided uniform Li plating. The Li||NCM811 cells can be cycled with limited Li (N/P=1) over 90 cycles. Additional advantage is that it improves the thermal stability of the NCM811 cathode.**

The demand for high-energy-density batteries has created a resurgence of interest in batteries with Li metal anodes because of their high specific capacity.<sup>[1,2]</sup> Nevertheless, the Li dendrites formation accompanied with the low coulombic efficiency (CE) hinder their practical applications. The low CE of Li deposition will cause active Li loss. Hence, In order to obtain long-term cyclability, this loss must be compensated by an excess of Li metal in the anodes (high negative/positive capacity ratio (N/P) – see **Table S1**), but the excessive Li compromises the high energy density of Li metal batteries.

The estimated energy densities of Li metal full cells when a Li anode is paired with various cathodes are given **Table S2**, which shows that, when a large excess of Li is paired with a  $\text{Li}_4\text{Ti}_5\text{O}_{12}$  cathode (**Refs. 1–5 in Table S1**), the energy density of a Li metal full cell is even inferior to the commercialized Li ion batteries. Consequently, to achieve the sought-after high energy density of Li metal full cells, one may need to replace the commercialized  $\text{LiFePO}_4$  with a high-voltage cathode (e.g.  $\text{LiNi}_{0.8}\text{Co}_{0.1}\text{Mn}_{0.1}\text{O}_2$ ). However, using the NCM811 cathode introduces other problems such as structural change due to the cation mixing<sup>[3,4]</sup>, oxygen evolution<sup>[5]</sup> and electrolyte decomposition<sup>[3,4]</sup>.

To address the issue of Li dendrites, research interests have been devoted to designing 3D conductive hosts<sup>[6–10]</sup>, nanoengineering at interphase<sup>[11–15]</sup>, optimizing the electrolyte<sup>[16–22]</sup> and applying the solid-state electrolyte<sup>[23–27]</sup>, but most of the strategies have been focused on the partial problems of Li metal anode. Although excellent performance has been achieved in Li||Li or Li||Cu half cells, the demonstrations of most Li metal full cells were usually obtained with cathodes below 4.0 V and excessive Li metal (See **Table S1** for comparison) With these approaches, the improved cycle life of the Li metal full cell is achieved at the cost of high energy density.

It is still challenging to find proper electrolyte that is compatible both with an aggressive high-energy-density cathode and with a high-efficiency Li metal anode. The low oxidation potential of ether-based electrolyte limits its application in Li metal batteries with aggressive high-voltage cathode, while the highly reactive nature of carbonate-based electrolyte with Li leads to low coulombic efficiency accompanied with sever dendrite formation. Recently, high-concentration ether-based electrolytes (HCE)<sup>[16–17]</sup> and localized high-concentration ether-based electrolyte<sup>[18–20]</sup> shows superior capability for high-efficiency Li metal batteries with high-voltage cathode. However, up to present, few papers have achieved stable cycling of Li metal batteries with limited Li or Cu foil in carbonate electrolyte.

Herein, we propose a strategy to achieve stable cycling of high-voltage Li metal batteries with high coulombic efficiency in carbonated-based electrolyte by optimizing the electrolyte composition with dual cations ( $\text{Li}^+$  and  $\text{Na}^+$ ) and ionic liquid (PP13TFSI). With this approach, stable Li deposition with high coulombic efficiency is achieved in carbonate-based electrolyte even with low-concentration lithium salt. Theoretical calculations and experimental investigation suggest that the salts and ionic liquid rather than the carbonate solvent in the optimized electrolyte are decomposed on the surface of Li metal anode to form cathode electrolyte interphase (CEI) and salt-rich solid electrolyte interphase (SEI). This not only protects the Li metal from the attack of carbonate solvent but also stabilizes the structure

<sup>a</sup> Department of Chemistry, Shanghai Key Laboratory of Catalysis and Innovative Materials, Center of Chemistry for Energy Materials, Fudan University, Shanghai, 200433, China

<sup>b</sup> Department of Chemistry, Chemical Theory Center and Minnesota Super-Computing Institute, University of Minnesota, 207 Pleasant street SE, Minneapolis, Minnesota 55455-0431, USA.

† Footnotes relating to the title and/or authors should appear here.

Electronic Supplementary Information (ESI) available: from the authors or RSC publishing

See DOI: 10.1039/x0xx00000x

NCM811 cathode. As a result, improved performance is achieved with the optimized electrolyte even with low N/P ratio. Additional advantage of the optimized electrolyte is that it improves the thermal stability of NCM811.

**Figure 1a** shows the CE of Li deposition in different electrolyte. The electrolyte containing 0.5 M LiPF<sub>6</sub>, 0.5 M LiTFSI, 0.2 M LiBOB and 0.15 M NaPF<sub>6</sub> in the mixed solution of propylene carbonate(PC), N-methyl-N-propylpiperidium bis(trifluoromethane-sulfonyl)imide (PP13TFSI), triethyl phosphate(TEP) and fluoroethylene carbonate(FEC) (1.5:1:1:0.5 in volume) shows the highest coulombic efficiency – over 97.5% and the longest cycle life – over 100 cycles, while the coulombic efficiency is below 80% in conventional LiPF<sub>6</sub> EC/DEC. The corresponding voltage profiles are given in **Figure S1**. We also measured the average CE of the Li deposition, which is over 99%, which is the highest determined by this method. (**Table S3**) For Comparison, the average CE in controlled electrolyte is 71.88%. (See **Figure S2** for details)

In the optimized electrolyte, with Na<sup>+</sup> ions in the electrolyte, the Li plating is more uniform. As schematically illustrated in **Figure 1b**, during the Li plating process, the electrical field drives both Li ions and Na ions in the electrolyte towards the Cu foil. Since the electrochemical potential of Na<sup>+</sup>/Na (-2.71V vs. SHE) is higher than that of Li<sup>+</sup>/Li (-3.04V vs. SHE), Na<sup>+</sup> will reduce into the Na metal seeds prior to Li<sup>+</sup> reduction. Due the

alloys, which bring about uniform Li deposition in the optimized electrolyte.<sup>[27]</sup> The Scanning Electron Microscope (SEM) during discharge confirms this process. Some particles are observed on the Cu foil after discharging to 0 V, we attributed this to the Na nucleus. In contrast, a smooth Cu surface is observed in the controlled electrolyte (**Figure 1c**). When 0.1 mAh cm<sup>-2</sup> Li is deposited on the Cu foil, obvious Li dendrite are found on the Cu surface in the controlled electrolyte, while a smooth surface with some Li-Na alloying particles are observed on the Cu surface in the optimized electrolyte (**Figure 1d**). When the deposition capacity increases to 1.0 mAh cm<sup>-2</sup>, a smooth and compact surface is obtained with optimized electrolyte, while large bulk of cracked and pulverized Li metals are observed on the Cu foil with controlled electrolyte. (**Figure 1e**) notably, no crack of the surface is found indicating the SEI layer is elastic. Further evidence of energy dispersive spectroscopy (EDS) mapping and the x-ray photoelectron spectrum (XPS) also confirm the process. (**Figure S3**) The Li metal retracted from NCM811 || Li full cells after 50 cycles also shows smooth and compact surface. (**Figure S4**) The characterizations of pristine NCM811 are given **Figure S5** and **Figure S6**.

**Figure 2a** shows the cycling performance of NCM811 || thick Li batteries operated under 3.0V to 4.3 V at 0.5 C. The initial discharge capacity is 142mAh g<sup>-1</sup>, which increases to 166 mAh

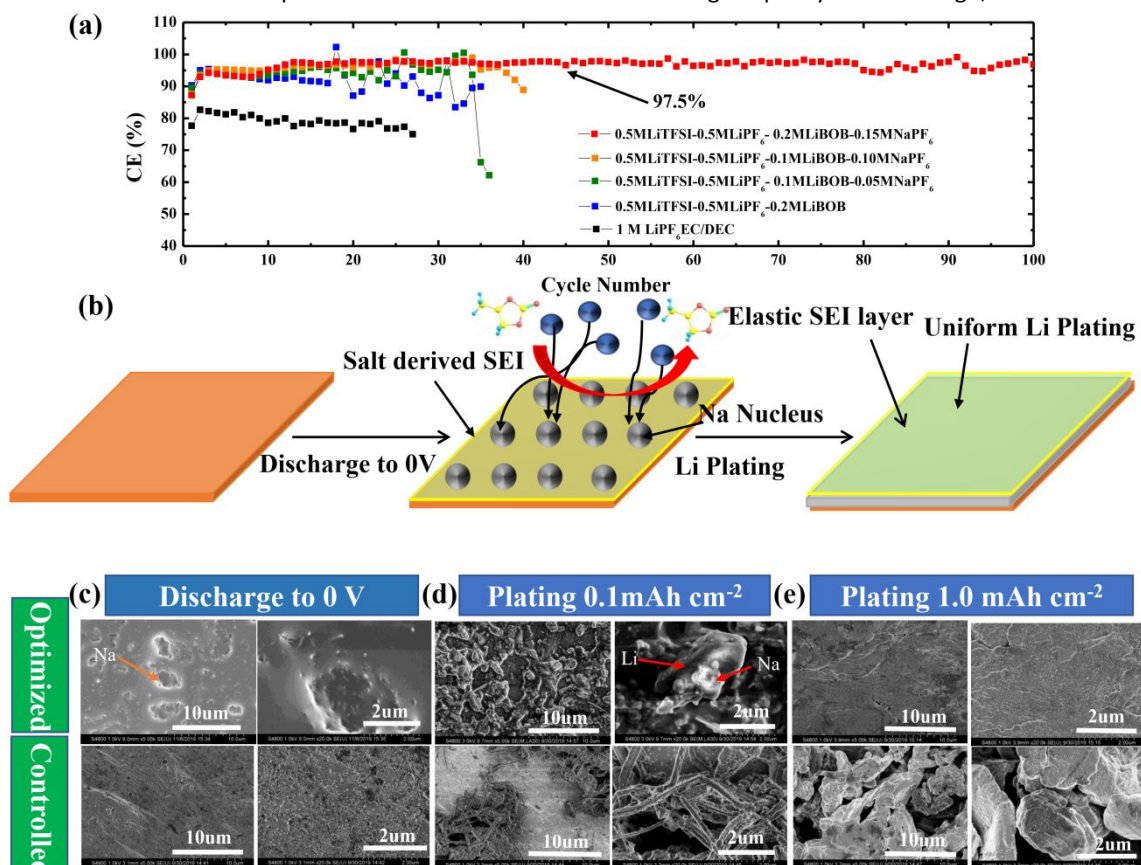
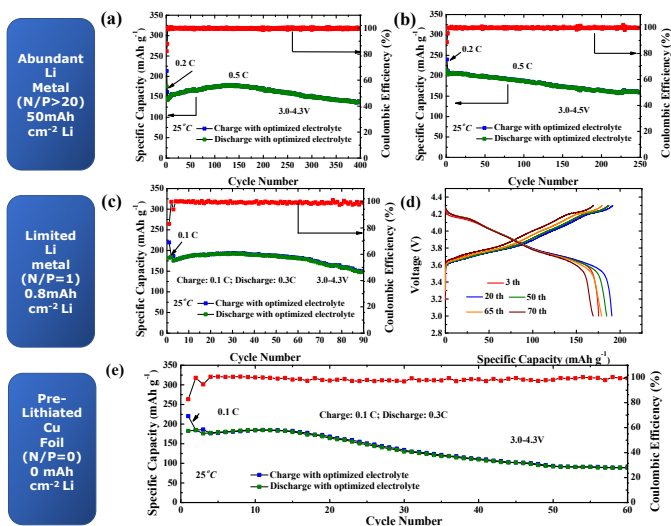


**Figure 1.** a) CE of Li | Cu half cells in different electrolyte; b) Schematic illustration of Li deposition process in the optimized electrolyte; c-e) morphology of Li deposition under different deposition capacity.

lithiophilic nature of Na, the subsequent adsorption of Li ions occurs preferentially on the Na metal seeds to form Li-Na

g<sup>-1</sup> after 150 cycles due to the gradual activation process. Even after 400 cycles, a specific capacity of 137 mAh g<sup>-1</sup> is still



achieved. When the cutoff charging voltage increases to 4.5 V, a high capacity of  $204 \text{ mAh g}^{-1}$  is obtained, which decreases to  $160 \text{ mAh g}^{-1}$  after 250 cycles. (Figure 2b) Figure 2c shows the cycling performance of NCM811||Li batteries with very limited Li ( $N/P = 1$ ,  $0.8 \text{ mAh cm}^{-2} \text{ Li}$ ). The battery shows an initial specific capacity of  $172 \text{ mAh g}^{-1}$ , which slowly increases to  $184 \text{ mAh g}^{-1}$ . After 90 cycles, a capacity of  $150 \text{ mAh g}^{-1}$  is achieved. The voltage profiles over selected cycles are given in Figure 2d, which shows that the polarization remains almost no change for 70 times. When a pre-lithiated Cu foil is paired with NCM811 in our electrolyte, a long cycle life of 60 with a capacity retention of 50% is achieved (Figure 2e). The corresponding voltage profiles are shown in Figure S7. The coulombic efficiency of the cell fluctuates between 97.3% and

99.2%. This performance in our carbonate-based electrolyte is comparable with what is achieved with HCE in ether-based electrolyte. The bare Cu was also employed for NCM811||Cu cells. (Figure S8) without pre-lithiation, the capacity decays much rapidly. The NCM811 with high loading is also tested, which also shows stable cycling performance. (Figure S9)

The surface chemistries of the Li metal anode and NCM811 cathode in the optimized electrolyte were investigated by theoretical calculations (Figure 3a).<sup>[28-29]</sup> The optimized molecular structures are given in Figure S10, and orbital energies of the HOMO and LUMO of the salts and solvents in the electrolyte are given in Table S4. Among all the salts and solvent molecules in the electrolyte, LiBOB, LiTFSI, LiPF<sub>6</sub>, LiNO<sub>3</sub>, NaPF<sub>6</sub> and PP13TFSI shows lower LUMO than the carbonate electrolyte, indicating these species are more likely to be reduced on the Li metal anode to form N, F, B, and P rich SEI layers, a carbonate-rich SEI layer is more likely to form in the controlled electrolyte. On the other hand, LiNO<sub>3</sub>, PP13TFSI, TEP, and LiBOB have higher HOMO energies than other components of the electrolyte, and this implies that those species are more likely than the other components to be oxidized. This will produce a CEI layer rich in N, P, and B, and the CEI layers in turn will inhibit the release of oxygen in the NCM811 and thereby help to stabilize the structure of the NCM811 cathode.

Figures 3b-3e and Figures 3f-3i shows the XPS spectra of both cathode and anode; the XPS spectra of other elements in the optimized electrolyte are given in Figure S11. Besides some new peaks (e.g., B-O bonding at  $\sim 198 \text{ eV}$ , Li<sub>3</sub>PO<sub>4</sub> at  $\sim 135 \text{ eV}$ ) arising from the salts in the optimized electrolyte, the major differences are observed in the C 1s spectra in both CEI layer and SEI layer. The peak intensity and peak area of C 1s on

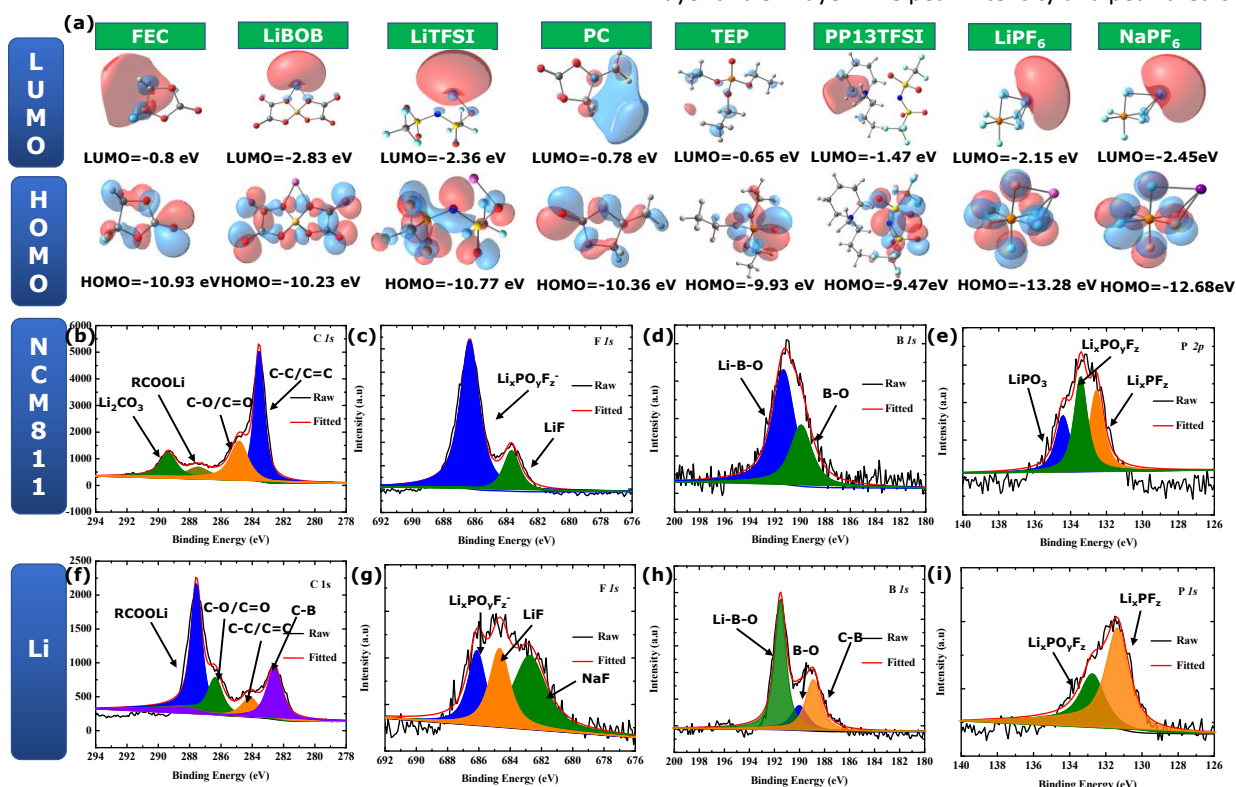


Figure 3. Surface chemistry of Li metal and NCM811 in the optimized electrolyte; a) theoretical calculation of frontier molecular orbitals of the salt and solvent in the optimized electrolyte; b-e) XPS spectrum of NCM811 cathode; f-i) XPS spectrum of Li metal anode.

both NCM811 and Li metal are much more intense in the controlled electrolyte (Figure S12) than in the optimized electrolyte (Figures 3b and 3f). This suggests that C species derived from the decomposition of carbonate solvent are more prevalent in the SEI and CEI in the controlled electrolyte than in the optimized electrolyte, and it suggests that the SEI and CEI in the optimized electrolyte mainly arise from the salt in the electrolyte rather than from the carbonate solvent. The stable SEI and CEI layers derived from electrolyte salts protect the Li metal from attack of carbonate solvent in the optimized electrolyte, which contributes to the high coulombic efficiency in the optimized carbonate-based electrolyte. Electrochemical Impedance Spectrum (EIS) on the Li||Li@Cu cell over cycles was also performed. (See Figure S13 and corresponding discussion). We also studied the microstructure by both high-

resolution transmission Electron Microscope (HRTEM) and SEM on cycled NCM811 cathodes. (See Figure S14 and S15 and corresponding discussions.) In addition, the Differential scanning calorimetry (DSC) result also demonstrates that the optimized electrolyte can enhance the thermal stability of NCM811 cathode. (See Figure S16).

In summary, we report the use of a carbonate-based electrolyte optimized with dual cations and ionic liquid to meet the challenges of high-energy-density Li metal batteries with aggressive high-voltage cathodes and very limited Li in the Li anodes. The electrochemical performance achieved by our optimized electrolyte can even be comparable to that of high-concentration ether-based electrolytes. Our work therefore points out a pathway for the future development of high-energy-density Li metal batteries.

### Conflicts of interest

There are no conflicts to declare. We acknowledge the fundings from the National Natural Science Foundation of China (No. 21875045), National Key Research and Development Program of China (2016YFB0901500), the Shanghai Science & Technology Committee (19DZ2270100) and the U.S. Department of Energy, Office of Basic Energy Sciences (DE-FG02-17ER16362).

### Notes and references

- X.B. Cheng, R. Zhang, C.Z. Zhao and Q. Zhang, *Chem. Rev.* 2017, **117**, 10403-10473.
- W. Xu, J.L. Wang, F. Ding, X. Chen, E. Nasybutin, Y. Zhang and J.G. Zhang, *Energy Environ. Sci.* 2014, **7**, 513-537.
- J. Kim, H. Lee, H. Cha, M. Yoon, M. Park and J. Cho, *Adv. Energy Mater.* 2018, **8**, 1702028.
- Y.K. Sun, S.T. Myung, B.C. Park, J. Prakash, I. Belharouak and K. Amine, *Nat. Mater.* 2009, **8**, 320-324.
- J. Wandt, A.T.S. Freiberg, A. Ogrodnik and H.A. Gasteiger, *Mater. Today* 2018, **21**, 825-833.
- X. Chen, X.R. Chen, T.Z. Hou, B.Q. Li, X.B. Cheng, R. Zhang and Q. Zhang, *Sci. Adv.* 2019, **5**, eaau7728.
- S. Yuan, J.L. Bao, C. Li, Y. Xia, D.G. Truhlar and Y. Wang, *ACS Appl. Mater. Inter.* 2019, **11**, 10616-10623.
- C. Zhang, R. Lyu, W. Lv, H. Li, W. Jiang, J. Li, S. Cu, G. Zhou, Z. Huang, Y. Zhang, J. Wu, Q.H. Yang and F. Kang, *Adv. Mater.* 2019, **31**, 1904991.
- H. Ye, Z.J. Zheng, H.R. Yao, S.C. Liu, T.T. Zuo, X.W. Wu, Y.X. Yin, N.W. Li, J.J. Gu, F.F. Cao and Y.G. Guo, *Angew. Chem. Int. Ed.* 2019, **58**, 1094-1099.
- J. Jia, Z. Tang, Z. Guo, H. Xu, H. Hu and S. Li, *Chem. Commun.* 2020, DOI:10.1039/D0CC00514B.
- Q. Cheng, A. Li, N. Li, S. Li, A. Zangiabadi, T. D. Li, W.L. Huang, A.C. Li, T. Jin, Q. Song, W. Xu, N. Ni, H. Zhai, M. Dontigny, K. Zaghbi, X. Chuan, D. Su, K. Yan and Y. Yang, *Joule* 2019, **3**, 1510-1522.
- X.L. Fan, X. Ji, F. Han, J. Yue, J. Chen, L. Chen, T. Deng, J. Jiang and C.S. Wang, *Sci. Adv.* 2018, **4**, eaau9245
- Y. Shuai, Z. Zhang, K. Chen, J. Lou and Y. Wang, *Chem. Commun.* 2019, **55**, 2376-2379.
- B. Shen, T.W. Zhang, Y.C. Yin, Z.X. Zhu, L.L. Lu, C. Ma, F. Zhou and H.B. Yao, *Chem. Commun.* 2019, **55**, 7703-7706.
- Q. Pang, X. Liang, I.R. Kochetkov, P. Hartmann and L.F. Nazar, *Angew. Chem. Int. Ed.* 2018, **57**, 9795-9798.
- L. Suo, Y.S. Hu, H. Li, M. Armand and L. Chen, *Nat. Commun.* 2013, **4**, 1481.
- J. Qian, W.A. Henderson, W. Xu, P. Bhattacharya, M. Engelhard, O. Borodin and J.G. Zhang, *Nat. Commun.* 2015, **6**, 6362.
- X. Cao, X. Ren, L. Zou, M.H. Engelhard, W. Huang, H. Wang, B.E. Matthews, H. Lee, C. Niu, B. Arey, Y. Cui, C. Wang, J. Xiao, J. Liu, W. Xu and J.G. Zhang, *Nat. Energy* 2019, **4**, 796-805.
- X. Ren, L. Zou, X. Cao, M.H. Engelhard, W. Liu, S.D. Burton, H. Lee, C. Niu, B.E. Matthews, Z. Zhu, C. Wang, B.W. Arey, J. Xiao, J. Liu, J.G. Zhang and W. Xu, *Joule* 2019, **3**, 1662-1676.
- P. Shi, H. Zheng, X. Liang, Y. Sun, S. Cheng, C. Chen and H. Xiang, *Chem. Commun.* 2018, **54**, 4453-4456.
- X.L. Fan, L. Chen, O. Borodin, X. Ji, J. Chen, S. Hou, T. Deng, J. Zheng, C. Yang, S.C. Liou, K. Amine, K. Xu and C.S. Wang, *Nat. Nano.* 2018, **13**, 715.
- S. Yuan, J.L. Bao, J. Wei, Y. Xia, D.G. Truhlar and Y. Wang, *Energy Environ. Sci.* 2019, **12**, 2741-2750.
- H. Huo, Y. Chen, R. Li, N. Zhao, J. Luo, J.G.P. da Silva, R. Mucke, P. Kaghazchi, X.X. Guo, X.L. Sun, *Energy Environ. Sci.* 2020, **13**, 127-134.
- C. Wang, L. Zhang, H. Xie, G. Pastel, J.Q. Dai, Y.H. Gong, B. Liu, E.D. Wachsman, L. Hu, *Nano Energy* 2018, **50**, 393-400.
- S. Choudhury, Z.Y. Tu, A. Nijamudheen, M.J. Zachman, S. Stalin, Y. Deng, Q. Zhao, D. Vu, L.F. Kourkoutis, J.L. Mendoza-Cortes, L.A. Archer, *Nat. Commun.* 2019, **10**, 3091.
- Y.X. Song, Y. Shi, J. Wan, S.Y. Lang, X.C. Hu, H.J. Yan, B. Liu, Y.G. Guo, R. Wen, L.J. Wan, *Energy Environ. Sci.* 2019, **12**, 2496-2506.
- J.L. Ma, F.L. Meng, Y. Yu, D.P. Liu, J.M. Yan, Y. Zhang, X.B. Zhang and Q. Jiang, *Nat. Chem.* 2019, **11**, 64-70.
- K. Leung, F. Soto, K. Hankins, P.B. Balbuena and K. L. Harrison, *J. Phys. Chem. C* 2016, **120**, 6302-6313.
- A. Wang, S. Kadam, H. Li, S. Shi and Y. Qi, *NPJ Comput. Mater.* 2018, **4**, 15.

An optimized carbonate-based electrolyte is proposed for the Li metal batteries with high-voltage cathode and limited Li metal.

